THE INFLUENCE OF AN IRON DEFICIENT DIET ON THE MURINE GUT MICROBIOME

by

Genevieve Lea Coe

A thesis submitted in partial fulfillment
of the requirements for the degree

of

Master of Science

in

Biochemistry

MONTANA STATE UNIVERSITY
Bozeman, Montana

May 2019

DEDICATION

This work is dedicated to my parents, Stanley and Elizabeth Coe.

Con cariño

TABLE OF CONTENTS

TABLE OF CONTENTS CONTINUED

LIST OF FIGURES

LIST OF TABLES

ABSTRACT

Iron is an essential nutrient for mammals[1]. It is involved in multiple redox reactions that are essential for the survival of most organisms[2]. There are two main types of iron that are absorbed from the diet: inorganic iron and heme[3]. Dietary iron ingested by mammals is mostly absorbed in the small intestine; however, it is unclear whether the gut microbiome is involved in iron homeostasis or whether iron in the diet influences the microbiome. The goal of this project is to characterize the change in microbial composition in response to iron deficiency and iron repletion in conventional mice and define a baseline model for future studies involving the more complex human gut microbiome.

THE IMPORTANCE OF IRON AS A NUTRIENT

Significance

Iron is the fourth most abundant metal in the earth's crust[1]. It is an essential nutrient for most organisms and is involved in critical biochemical reactions involving electron transfer. These reactions include oxygen transportation in mammals involving the tetrapyrrole heme bound by hemoglobin for oxygen transport in red blood cells, cytochrome c involved in electron transfer for oxidative phosphorylation, and hydrogen peroxide degradation by catalase (**Figure 1**)[2].

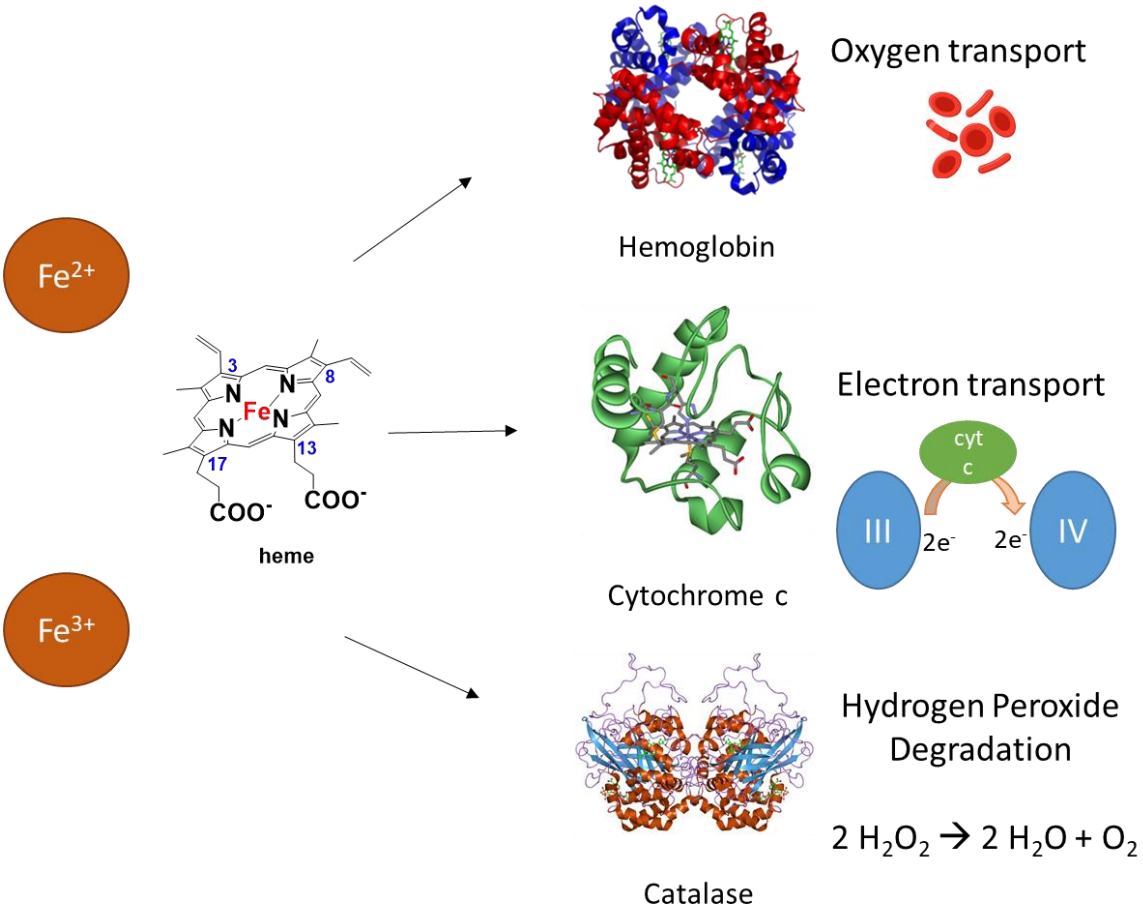

Figure 1. Iron is an essential nutrient to multiple biochemical processes in the body. Iron exists in multiple forms (inorganic or heme) and is used primarily within heme to carryout important redox reactions in the body including oxygen transport in hemoglobin, electron transport during oxidative phosphorylation to make ATP, and degradation of harmful hydrogen peroxide species by catalase.

Iron In The Diet

Bioavailability of Iron in Mammals

Almost all organisms require iron to meet daily needs for important biochemical processes. However, the mechanism for iron metabolism is unique compared to other metal nutrients because there is no distinct physiological pathway for cellular excretion[3]. Most daily needs are met by recycling iron from red blood cells, and sequestration from iron stores when necessary, but over time, iron is lost through sweating and sloughing of dead cells. In addition to recycling, iron is repleted from the diet. Most humans absorb 1-3 mg of iron per day to make up for lost iron[3]. While iron is an essential nutrient, it is also toxic if not strictly regulated. Several studies have demonstrated oxidative damage in various cell types and tissues caused by disrupted regulation of iron levels [4]. Iron is a d-block metal and can stably exist in two oxidation states (Fe^{2+}, Fe^{3+}) [1]. In most organisms, the valency of iron depends on the physiological pH of the surrounding environment. Iron is ingested both in the ferric, Fe(III), and ferrous, Fe(II), states but can only be absorbed into a mammalian cell in the ferrous form. Daily iron intake is mostly comprised of inorganic iron but only a small percentage is absorbed by mammals[3]. In contrast, a large fraction of absorbed dietary iron in mammals comes from heme (~30-40%), a tetrapyrrole with an iron center (**Figure**

1), suggesting it is more efficiently metabolized and hence more intrinsically bioavailable [3]. Dietary heme is commonly obtained from consumption of red meats, fish, and some legumes, but even though it is a very efficiently absorbed source of dietary iron, the mechanisms of cellular uptake and transport have yet to be characterized.

Mammalian Iron Absorption

Most dietary inorganic iron absorption in mammals occurs in the duodenum of the small intestine, where there are multiple routes of entry into the cell; each requiring an extracellular ferric reductase and divalent metal transporter. Two well characterized iron transport mediators in the small intestine are Dcytb (CBYRD), a ferric iron reductase, and Dmt-1 (SLC11A2) or divalent metal transporter-1, which together, transports ferrous iron into the cell. Once inside, ferrous iron can either be stored in ferritin, an intracellular iron storage protein, or it can be exported by ferroportin (SLC40A1), where it is then bound by transferrin for transport through the blood stream to other tissues (**Figure 2**). The precise mechanisms of cellular heme uptake and transport are unclear, but it has been reported that the majority of dietary heme is absorbed in the large intestine indicating that there are other mechanisms of dietary iron regulation depending on the source[5].

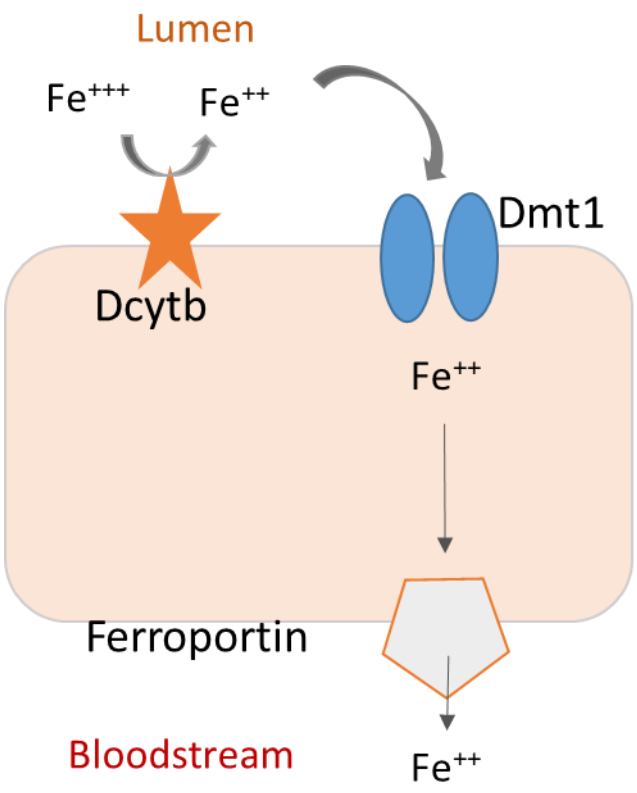

Figure 2. Major iron biomarkers involved in iron absorption in the small intestine. An extracellular iron reductase like Dcytb is required for reduction of ferric iron (Fe(III)) to ferrous iron (Fe(II)) before it can be transported across the cellular membrane by Dmt-1. Once inside the cell, iron can be bound by ferritin for later use(not shown) or exported into the bloodstream to transferrin(not shown) by ferroportin, the only known transmembrane iron transporter.

Regulation of Iron

Multiple tissues and organs are involved in the tight regulation of iron homeostasis (**Figure 3**). Once in circulation, plasma transferrin-bound iron can be taken to bone marrow for use in erythrocytes (red blood cells) production; it can be recycled in the spleen by macrophages; or it can be stored in liver hepatocytes for later use[6].

Within the major centers of iron metabolism in the body, there are important hormones, proteins, and metabolites that influence iron flux. For example, hepcidin, a hepatic hormone, is critical for iron absorption and circulation[6]. It controls the expression of ferroportin and inversely regulates iron uptake and export in the duodenum[6]. Other factors influencing regulation of physiological concentrations of iron include diet, genetic factors, and inflammatory diseases.

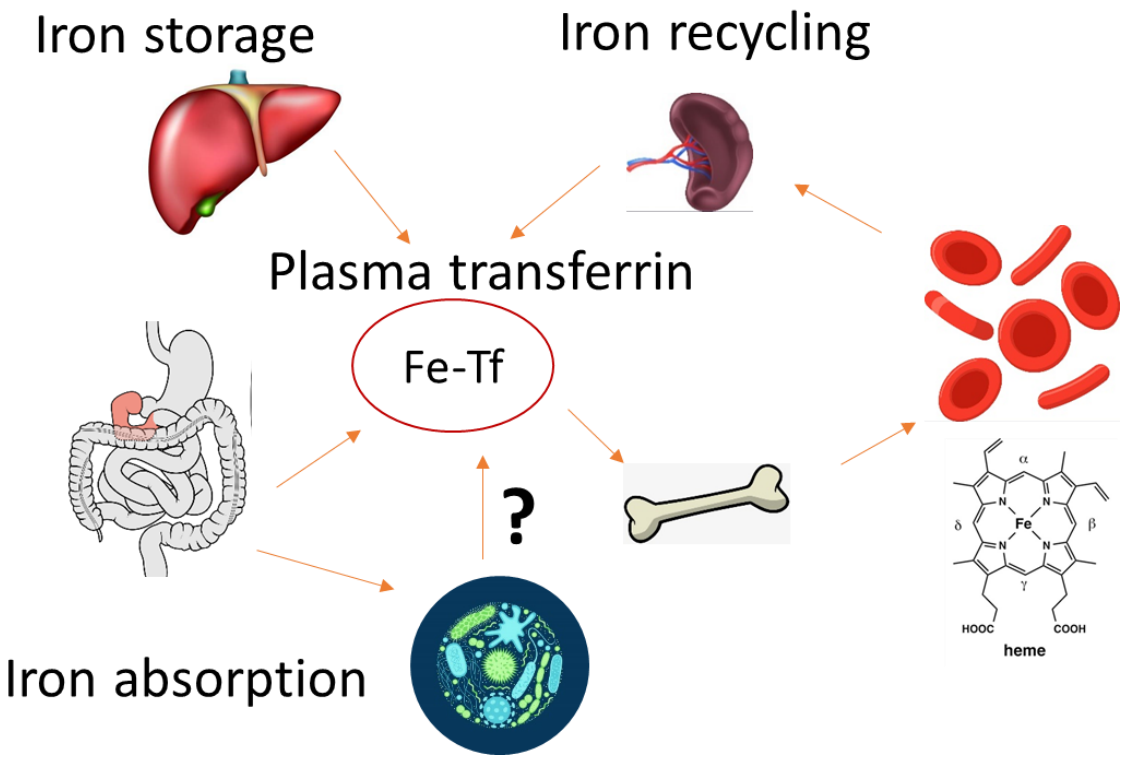

Figure 3. Pathways of mammalian iron regulation. Plasma transferrin bound iron (found in the bloodstream), can circulate iron to various tissues depending on the needs of the host. It can be taken to bone marrow for production of erythrocytes (red blood cells), which use iron in the form of heme for oxygen circulation after which it can be recycled in the spleen by macrophages. Iron can also be stored in the liver after it is absorbed from the duodenum or after is has been recycled from the spleen. The role of the microbiome on host iron regulation in the gut is currently unclear.

Dietary Factors Influencing Iron Bioavailability

Dietary factors negatively influencing the absorption of iron in the intestine include phytates from plants, polyphenols from wine, coffee, tea, some cereals and legumes, calcium and several milk-based proteins. These have all been referenced in the literature to be inhibitors of iron absorption mainly by inhibiting the reduction of ferric iron to the absorbable ferrous form[7]. Dietary iron overload has also been demonstrated to disrupt iron regulation by inhibiting signaling pathways for iron uptake and transport[8,9]. On the other hand, iron deficient diets are the leading cause of iron deficiency anemia, which is thought to affect 126 million people worldwide[10]. As described below, the gut microbiome may also play a key role in host iron regulation.

Significance of the Mammalian Gut Microbiome in Iron Bioavailability

The mammalian gut microbiome is comprised of billions of microbial cells throughout the GI tract[11-13]. Many studies in recent years suggest these microbes, mainly bacteria, promote the integrity of the intestinal tract, aid in nutrient metabolism, and regulate overall host health[13-17]. Fe studies have addressed whether the gut microbiome and the factors influencing its composition, influence host iron bioavailability. As such, the role of the gut microbiome in host iron metabolism remains unclear.

Iron Acquisition by Gut Bacteria

The majority of the gut microbiome is comprised of bacteria, most of which require iron. As mentioned previously, the bioavailability of iron in the mammalian GI tract is dependent on source and environmental pH. The most common method of iron acquisition by gut bacteria from a mammalian host involves the production of siderophores, small molecule iron chelators that bind extracellular Fe(III) with a high affinity and are reabsorbed into the bacterial cell by extracellular proteins that recognize individual siderophores[18-20]. The acquisition of iron by siderophores produced from gut bacteria can have a major influence on iron bioavailability for the host, suggesting that a better understanding of the relationship between host and gut microbiome regarding iron metabolism may lead to novel therapies for treating anemia. Additional mechanisms of bacterial iron acquisition include the expression of outer membrane receptors for host plasma transferrin bound iron and hemophore molecules for binding host heme bound proteins[20]. Both commensal and pathogenic strains of bacteria implement some of the same mechanisms for host iron acquisition[21]. Some species of commensal gut bacteria have been shown to protect the host from pathogenic invasion by iron sequestration strategies[18]. The mammalian host also has mechanisms in place to sequester iron from pathogenic iron scavengers[22]. It has been reported in the literature that many pathogenic bacterial infections, involving *S. aureus*, *C. difficile*, *P. aeruginosa*, and *S. enterica* to name a few, are dependent on host iron supplies in order to colonize and spread[23-25]. It is still unclear how iron in a mammalian host is regulated to meet the needs of both host and commensal gut microbiota. Understanding the critical factors

influencing iron bioavailability can lead to development of potential probiotics and therapeutics for treating iron deficiency anemia and pathogenic infections.

Gap in the Knowledge

In this study, we used conventional C57B1/6 mice to study the influence of dietary iron deficiency and subsequent iron repletion on the gut microbiome. Past studies examining the gut microbial contents of lab mice and humans have shown that the anatomy of both mammals is similar and the composition of the intestinal microbiota at the phylum level are both predominantly comprised of bacteroidetes and firmicutes[26,27]. However, the physiology of mice differs significantly from humans in terms of metabolic rate and nutritional requirements as well as gut microbial consortium at the family level and below. The model constructed here has been characterized to account for the difference in rate of iron metabolism in mice and their dietary intake and deficiency of iron has been adjusted to better reflect the total average iron found in humans[28]. Male and female mice, both young and age-matched and mature, were switched from a standard chow (see materials and methods) to a double irradiated, iron deficient chow for the duration of each experiment. In this way we were able to account for dietary iron consumption. Initial experiments looked at mice sustained on the deficient chow with 50 ppm $FeSO_4$ supplied in their water for two weeks followed by two weeks of iron deficient chow and purified water. This concentration of iron was chosen to reflect the total amount of iron in an average human host. It was cited by another group to allow for changes in the murine host response to iron variation to be detected. The 290 mg iron/kg dry weight in their standard chow has been reported to

mask the host response when dietary iron availability was reduced or increased. Iron metabolism at the systemic and excretion level were monitored during this time and intestinal tissues were harvested upon sacrifice to analyze expression of major iron biomarkers in the duodenum and cecal tip. Following experiments were carried out repeating the phases described above followed by an additional two weeks of iron repletion after iron deficiency (0.32 mM $FeSO_4$ x 7 H_2O supplied in the water). Systemic and excreted iron was monitored by ICP-MS (Inductively Coupled Plasma-Mass Spectrometry) and intestinal tissues were collected upon sacrifice. Fecal pellets for all experiments were split and used for 16s rRNA sequencing to analyze the gut microbiome adaptation to each phase of iron treatment. By allowing two weeks for each phase we were able to determine that mice were feeling iron deficient and whether they were able to be restored to healthy iron levels by using a defined iron source. Future studies done in our lab will use this characterized mouse model as a host environment to study the influence of iron bioavailability on more complex human gut microbiota using two defined iron sources ($FeSO_4$ and heme). We performed a pilot study using heme as an iron repletion source instead of iron sulfate. Results from this study can be found in the appendix. We are currently working on optimizing the experimental approach using heme as a repletion source to ensure that mice are receiving the correct amount of total iron so that results can be compared to iron sulfate repleted mice in the future.

EXPERIMENTAL APPROACH

Mouse Husbandry and Administration of Iron Deficient and Iron Supplemented Diets.

Conventional C57Bl/6 mice used in this study were bred and raised in-house at the Animal Facility at Montana State University, Bozeman, MT. A total of 4 cohorts of female mice and 3 cohorts of male mice housed in groups of 5 were sustained on a standard chow (Autoclavable rodent breeder diet 5013 from Labdiet, St Louis, MO, 290 mg iron/kg dry weight chow) for 6-10 weeks until the first day of dietary iron treatment when they were switched to an iron deficient chow (U8958 version 176, from SAFE Augy, France, 4 mg iron/kg dry weight chow). All mice were fed the iron deficient chow for the duration of the experiment. See below for a detailed description of mouse cohorts. Iron treatment started with 45.7 mg iron sulfate heptahydrate dissolved in 500 mL purified water for two weeks, allowing time for the mice to adjust to the new diet. Mice were then switched to iron-free, purified water for the following two weeks, during which their serum and fecal pellets were collected and monitored for signs of anemia. Two cohorts of female mice were sacrificed and tissues harvested to analyze the host response to iron deficiency at this point. The remaining cohorts were supplied with either 0.32 mM iron sulfate (Iron(II) sulfate heptahydrate from Acros Organics) or 0.076 mM hemin chloride (Calbiochem) (see appendix) for two weeks before sacrifice (equates to 50 mg/L of either iron source) to analyze the host and microbial response to dietary iron repletion.

Mouse Cohorts Used in Iron Deficiency and Repletion Experiments

In order to assess the conventional mouse response to dietary iron deficiency and repletion, a total of 7 cohorts of mice were characterized for host and gut microbial response to iron treatment.

Group 1: Female C57Bl/6 mice (9 weeks old) used in adaptation to iron deficiency phase. 10 female C57Bl/6 conventional mice raised in house at Montana State University were switched from a standard mouse chow (250 mg/kg total iron) to and iron deficient chow (4 mg/kg total iron) with 0.32 mM iron sulfate heptahydrate supplemented in their water at 9 weeks of age. After a two-week period on this diet, mice were switched to purified water and remained on the iron deficient chow (4 mg/kg total iron) for a following two-week period. Mice were sacrificed according to AARC guidelines and tissues were collected for iron biomarker analysis. Blood and fecal pellets were collected throughout the duration of the experiment at time points described in the main text to analyze total iron retention, excretion, and gut microbial composition.

Group 2: Female C57Bl/6 mice (9 weeks old) used in adaptation to iron deficiency and repletion phases. 10 female mice raised in house at Montana State University were switched from a standard mouse chow to an iron deficient chow with 0.32 mM from iron sulfate heptahydrate supplemented in their water at 9 weeks of age. Mice were switched to purified water and remained on the iron deficient diet (4 mg/kg total iron) for a following two week period. 5 mice were then supplemented with 0.32 mM iron sulfate heptahydrate in their water for the final two weeks of the experiment after which they were sacrificed and tissues harvested for further analysis. The remaining 5 mice were

supplemented with 0.076 mM from hemin chloride to assess the host and gut microbiome response to iron repletion using a different source of iron (see appendix). Blood and fecal pellets were collected according to the protocol described below.

Group 3: Male C57Bl/6 mice (15 weeks old) used in adaptation to anemia and iron deficiency phases. 5 male mice raised in house at Montana State University were switched from a standard mouse chow to an iron deficient chow with 0.32 mM iron sulfate heptahydrate supplemented in their water at 15 weeks of age. Mice received the same diet regimen for adaptation to anemia and iron repletion as previously described above. Blood, fecal pellets, and tissues were harvested and processed as described below. We used older male and female mice as they became available to further assess gender and potential age differences and reduce live specimen waste.

Group 4: Male C57Bl/6 mice (10 weeks old) used in adaptation to anemia and iron repletion phases. 5 male mice raised in house at Montana State University were switched from a standard mouse chow to an iron deficient chow with 0.32 mM iron sulfate heptahydrate supplied in their water at 10 weeks of age. Mice were maintained on the iron specified diet described previously and samples were collected as described below.

Group 5: Female C57Bl/6 mice (11 weeks old) used in adaptation to iron deficiency phase. 5 female mice were maintained on the iron specified diet for adaptation to iron deficiency phase as described for group 1 mice. The purpose of repeating this phase was to collect small intestinal tissues that were damaged in processing from group 1 mice.

Group 6: Female C57Bl/6 mice (11 weeks old) used in adaptation to iron deficiency and repletion phases. Group 6 mice followed the same diet regimen as described for group 2

mice. This experiment was repeated in order to statistically analyze the trends in host and microbial adaptation to iron deficiency and repletion in male and female conventional mice.

Group 7: Male C57Bl/6 mice (10 weeks old) used to monitor gut microbial stability in response to initial switch in chow. 5 male mice were switched to the iron deficient chow at 10 weeks of age for a period of 3 weeks. Diet is a significant factor influencing the gut microbiome. Fecal pellets were collected three times a week and processed for 16S rRNA analysis in order to assess the time required for the conventional mouse microbiome to stabilize after being switched to the iron deficient chow. It was determined that the gut microbiome stabilizes before the two week period of iron deficiency commences (data not shown).

Preparation of Serum and Pellet Samples for Total Iron Quantification.

Serum samples were collected weekly according to AARC guidelines for blood draws (<60 μL) and stored at -20 ^{0} C until prepared for total iron quantification using inductively coupled plasma-mass spectrometry (ICP-MS). *Serum:* Blood was thawed at room temperature and centrifuged (accuSpin micro R, Fischer Scientific) for 10 min at 1,677 x g to separate serum. 20 uL of serum was pipetted off the top of each sample and incubated in 1 mL of 50% nitric acid (Nitric Acid optima and trace metal grades, Fischer Chemical) at 55 ^{0} C for 30-60 min or until dissolved. Samples were diluted with 9 mL of metal free water (Millipore) and centrifuged at 5700 x g for 10 min (Beckman Coulter J2-MI). After centrifugation, samples were sterile filtered (0.2 uM Corning syringe filters)

and stored in the dark at room temperature until analysis. Fecal pellets analyzed for total iron were collected each week on the day of and approximately 24 hours after a change in diet regimen. Data shown below represents pellets that were collected 24 hours after a change in diet except for the day of sacrifice (two weeks of iron repletion). Pellets were dried overnight using vacuum suction and weighed before being incubated with 1 mL 50% nitric acid at 55 ^{0} C for 1 h. Samples were diluted with 9 mL metal free water and centrifuged at 5700 x g for 10 min before filtration to remove particulates. All samples were stored in the dark at room temperature until analysis by ICP-MS.

Total Iron Quantification from Murine Serum and Pellets Using ICP-MS.

Samples were prepared as described above and measured on an Agilent 7500ce ICP-MS used with a collision cell and a certified environmental calibration standard from CPI International (Product No. 4400-12 1116NCO2). Total iron per sample after instrument analysis was calculated based on volume (serum) or dry mass (pellets).

RNA Extraction of Murine Tissues.

Tissues were immediately harvested from sacrificed mice and snap-frozen in liquid nitrogen and stored at -80 ^{0} C. Duodenum and cecal tip tissues were thawed on ice, split in half, and immediately processed for RNA extraction using a mini-RNA extraction kit from Qiagen (Germany). Tissue lysis was carried out with manual grinding using a pestle, water bath sonication (Fisher Scientific; program: pulse 10s on, 10s off, 80% amplitude for 2 minutes), and shredding using Qiagen Qiashredder tubes. RNA was

quantified using a nanodrop (ND-1000, NanoDrop Spectrophotometer) and stored at -80^{0} C until further use.

Design of Primers for Iron Biomarker Analysis.

Mouse primer sequences adapted from Deschemin et Al. include Dcytb and Ferroportin[29]. Mouse Dmt-1 and β-actin were acquired from the NCBI primer-BLAST library. All primer sequences (Table 1) were analyzed for integrity using NetPrimer software from Premier Biosoft. Integrity is assessed by the location of the primer on the operon, the complementarity of the forward and reverse sequences, melting temperature (GC content) and to ensure that there is no redundancy in sequences which might cause the formation of primer dimers (annealing of primers to each other). Primers were synthesized at Integrated DNA Technologies (Coralville, IA).

Amplification of Iron Transporters by qPCR.

cDNA was synthesized by reverse transcription of mRNA using iScript polymerase master mix from BioRad (Hercules, CA) and a 2720 thermal cycler from Applied Biosystems (program steps: 25 °C for 5 minutes, 46 °C for 20 minutes, 95 °C for 1 minute, 4 °C hold). Amplification of cDNA by qPCR was performed on a Roche 96 Light Cycler from Roche Diagnostics (Switzerland) using the preset program for SYBR green fluorescent dye. Reactions were prepared with AzuraQuant Green Fast qPCR mix (LoRox) from Azura Genomics (Raynham, MA). Amplification of cDNA was semi-quantified relative to the control, β-actin, using Roche Light Cycler software v.1.5 and fold change was quantified using the ΔΔCt method and plotted in GraphPad Prism v.7.

Preparation of DNA from Fecal Pellets for 16S rRNA Sequencing.

Pellets were collected on the day of and 24 hours after a change in diet regimen (except for the two week repletion, which was collected on the day of sacrifice) and split for total iron quantification and DNA analysis. DNA extractions were carried out using a Qiagen DNeasy Powersoil kit following manufacturer's instructions. DNA was stored at -20 ^{0} C until time of data acquisition. Sequences were amplified from the V4 region of the 16S rRNA encoding gene at the University of Michigan Center for Microbial Systems using Illumina MiSeq 2 x 250bp paired-end sequencing.

Analysis of 16S rRNA Sequencing Output.

Pellets were collected from conventional mice on the first day of iron treatment and every week after for the duration of treatment as described previously. DNA extracted from pellets each week was sent to the University of Michigan for sequencing of the V2 region of the 16S ribosome. Sequences were downloaded from the Illumina database and compiled into operational taxonomic units (OTUs) using mothur v.1.39.5. OTUs were filtered and compiled into a table corresponding to each mouse. NMDS plots for β-diversity, inverse-simpson to show α-diversity, and taxonomy charts were compiled in R version 3.5.1 using vegan and labdsv packages with custom scripts.

Statistical Analysis

Significance in mean variance of α-diversity was calculated in R using Welch's two tailed t-test. Significance of treatment and gender factors on microbiome clustering was determined using PERMANOVA analysis (adonis2) in R. Significance between treatment phases for all groups of mice (baseline, anemia, repletion) regarding host response was calculated in GraphPad Prism using wilcoxon's unpaired t-test. Significance of effect size between treatment groups regarding the gut microbiome response was calculated using indval.

INFLUENCE OF IRON BIOAVAILABILITY ON THE MAMMALIAN GUT MICROBIOME

Introduction

Both mammalian host and gut microbiome require iron to satisfy metabolic needs[1]. Most iron in the mammalian host is tightly regulated and repletion of lost iron occurs only through the diet[2]. Previous studies have suggested the potential role of the gut microbiome in dietary iron metabolism in mammalian hosts but the influence of iron bioavailability on the composition and stability of the gut microbiome is not fully understood. Here we characterized the male and female conventional mouse response to dietary iron deficiency and repletion. We then analyzed the gut microbial response to iron bioavailability. Conventional mice (C57Bl/6) have been shown in the literature to have similar gut microbiome compositions (at the phylum level) and are able to efficiently colonize human gut samples. We plan to use this model for further studies looking at the adaptation of human gut microbiota colonized in the C57Bl/6 mouse.

Results

Host Response to Iron Deficiency and Repletion in C57Bl/6 Mice.

Total iron was quantified by ICP-MS from serum and pellets collected at the end of each of the 4 weeks of the experiment for mice given an iron challenge (group 1) and then sacrificed, or at the end of 6 weeks for mice rendered anemic and then repleted with inorganic iron ($FeSO_4$) (groups 2-4). Averages in total iron were obtained based on

cohort and iron treatment. The concentration (males and females) of iron circulating in blood (systemic iron) over the 4 or 6 week course of iron treatment did not fluctuate significantly within each cohort (**Figure 4A,** Table 2a-c). Total iron from fecal pellets in iron deficient mice (**Fig 4B**) decreased in each cohort (Table 3a-c). These results suggest that the host recycles systemic iron during the period of dietary iron deficiency in order to satisfy systemic needs. Systemic iron increased slightly in females (group 2) and remained level in both groups of males upon repletion with iron sulfate (**Fig 4C**), however, there are more dramatic differences in excreted iron between male and female cohorts on the first week of repletion (**Fig 4D**). These differences could be explained by gestational periods in females as well as different systemic iron needs between male and female mammals. The amount of fecal iron increased after one week of iron repletion to near-baseline level in all cohorts (Table 3a-b).

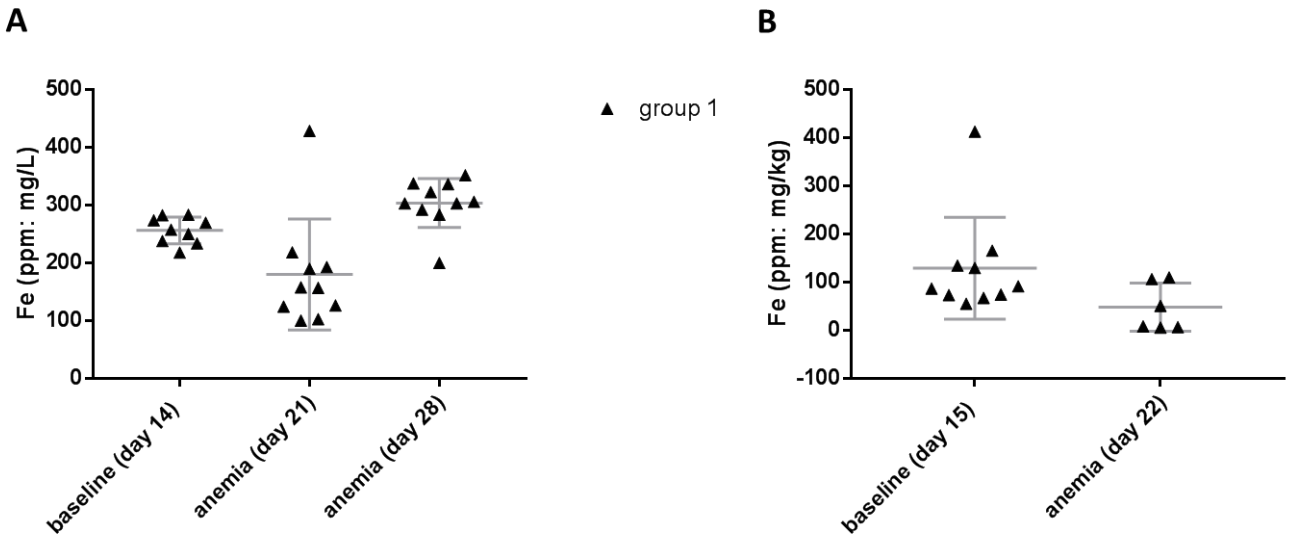

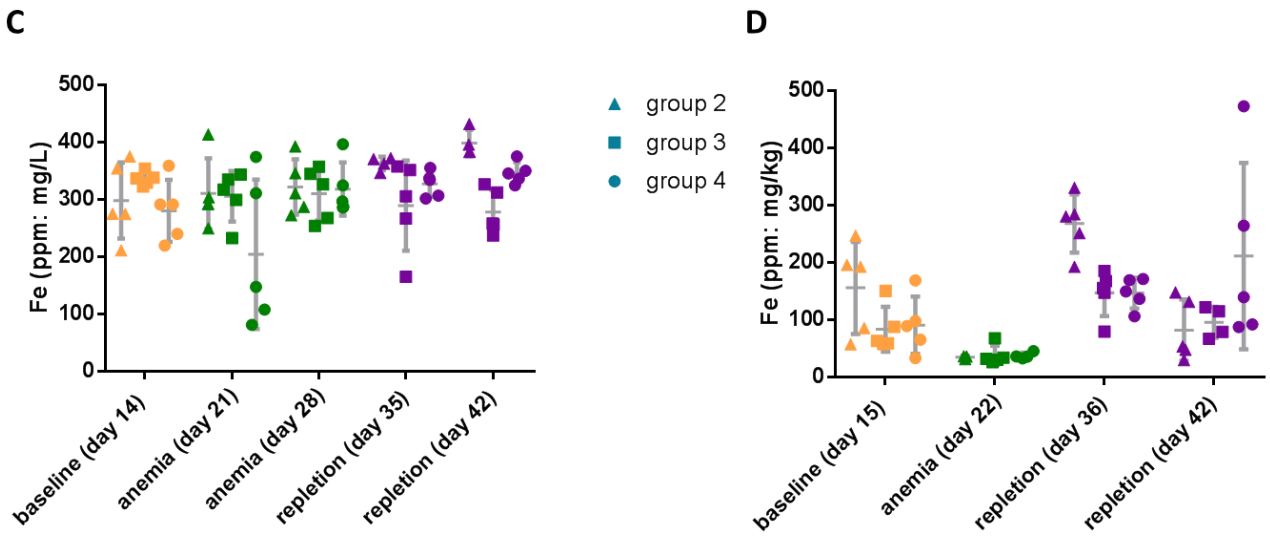

Figure 4. Systemic iron does not fluctuate in response to iron deficiency while excreted iron decreases (deficiency) and increases (repletion). A) Total iron quantified from conventional mouse serum over the course of iron deficiency (group 1). B) Total iron quantified from conventional mouse pellets over the course of iron deficiency (group 1). C) Total iron quantified in serum over the course of iron deficiency and repletion (groups 2-4). D) Total iron quantified from pellets over the course of iron deficiency and repletion (groups 2-4). Colored triangles and squares represent female and male mice, respectively, (groups 2-4). Error bars represent one standard deviation from the mean, which was calculated separately for males and females in each phase.

In addition to quantification of total iron, iron-responsive biomarkers from two regions of the small intestine, the duodenum and cecal tip, were amplified by qPCR from anemic and iron-repleted mice. The duodenum represents the area from which nutrients

are principally absorbed, while the cecal tip is a microbe-rich pouch protruding from the region where the small intestine meets the ascending colon. The iron biomarkers chosen are reported to be regulated by iron at the transcriptional level[29-31]. Upregulation of these markers as iron availability becomes scarce indicates that the host is in early stages of iron deficiency anemia. Expression of iron biomarkers was calculated from the number of cycles in qPCR required to amplify above the baseline relative to the amplification of the mammalian housekeeping gene, β-actin. Fold-change of iron transporter transcripts was calculated relative to two conventional male C57Bl/6 mice sustained on a standard chow consisting of 250 ppm iron. Expression of iron transporters in the duodenum and cecal tip of 5 female mice (group 5) depleted of dietary iron for two weeks showed upregulation in fold change (duodenum, mean ± sd: Dmt1-66 ± 18, ferroportin-17 ±5, Dcytb-32 ±22; cecal tip: Dmt1-298 ±93, ferroportin-134 ± 44, Dcytb-318 ± 183) of all transcripts, suggesting that the mice are in early stages of iron deprivation (Table 4a, 5a, **Figure 5A,B**). Notably, the fold-change values observed here vary in magnitude according to both the particular biomarker used and the region of the GI tract sampled, for reasons to be discussed below.

Transcripts of the same biomarkers from mice following repletion with iron sulfate in male and female mice (groups 3, 4, 6) were lower in fold change expression. Both male (groups 3-4) and female mice (group 6) repleted with iron showed reduced fold change expression of iron biomarkers in the cecal tip compared to iron deficient

mice (group 5) (**Figure 5C,D,** Table 4b, 5b).

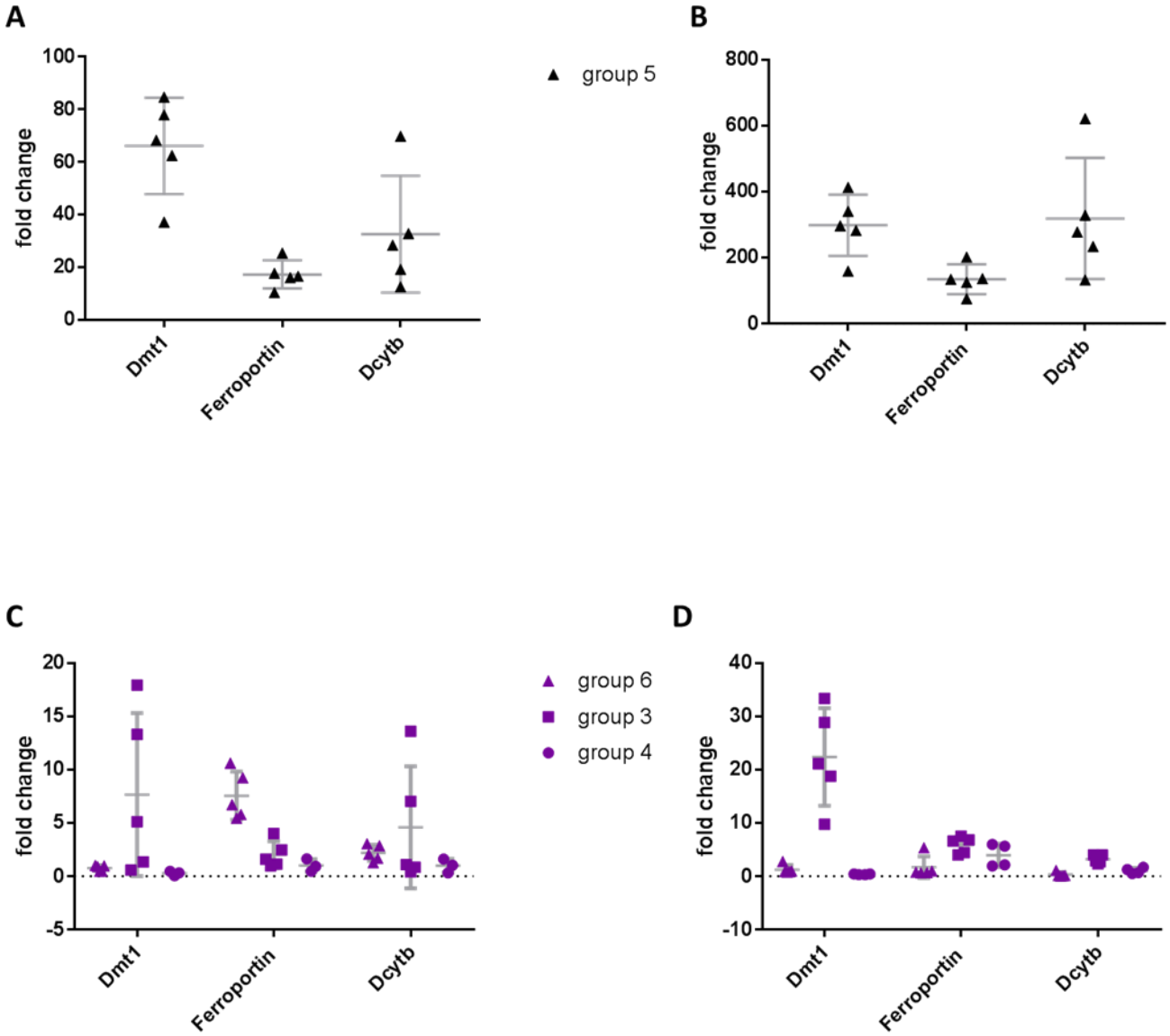

Figure 5. Fold-change of iron biomarkers in the small intestine of female iron deficient mice are elevated compared to iron repleted mice. Fold change expression of iron transporters in the A) duodenum and B) cecal tip of iron deficient mice (group 5). C) duodenum and D) cecum of iron repleted male and female mice (groups 3,4,6). Colored triangles and squares represent female and male mice, respectively (groups 3, 4, 6). Error bars represent one standard deviation from the mean, which was calculated for males and females separately for each treatment phase.

The Microbiome Decreases in Diversity
in Response to Dietary Iron Deficiency in C57Bl/6 Mice.

Over the two-week period of iron deficiency, there is a decrease in α-diversity of the conventional mouse gut microbiome (**Figure 6A,B**). α-diversity describes the spread of the microbiome in terms of richness and evenness, where richness indicates the number of different operational taxonomic units (OTUs) or unique bacterial sequence reads in the microbiome and evenness indicates the abundance of each OTU. β-diversity plots (**Figure 6C,D**) of groups 1 and 5 mice show the gut microbiome diversity of each mouse (represented by one dot) in relation to other mice within and between each phase of iron treatment. A similar shift is seen relative to α-diversity where the diversity of the gut in each mouse is more similar within a phase of iron treatment than it is between phases. Mice cluster more closely together during iron deficiency, supporting the decrease in diversity seen in **Figure 6A,B**. Diversity and taxonomy plots were generated with mouse groups 2-6 where T0 = day of the switch from standard chow (250 mg/kg iron) to the iron deficient chow and 0.32 mM iron sulfate heptahydrate supplemented in the water, baseline = 7 and 14 days of iron deficient diet + 0.32 mM $FeSO_4$ x $7H_2O$, Anemia = 7 and 14 days after the switch to iron free water, Repleted $FeSO_4$ x $7H_2O$ = 7 and 14 days after iron repletion with 0.32 mM iron sulfate heptahydrate. Repletion with a defined iron source ($FeSO_4$) results in an increase in α-diversity in iron sulfate fed mice (**Figure 6E-H**).

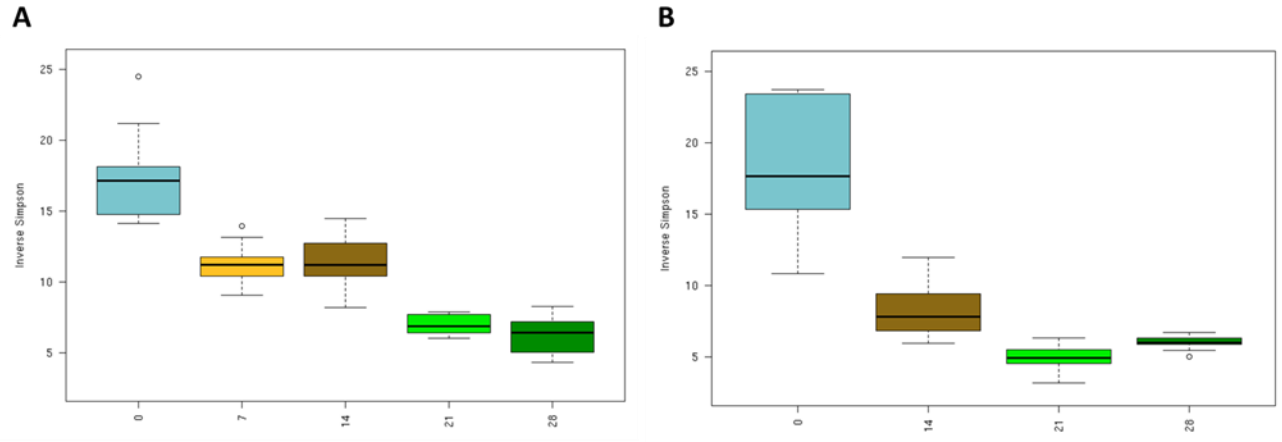
A
Inverse Simpson
25
20
15
10
5
0
7
14
21
28
B
Inverse Simpson
25
20
15
10
5
0
14
21
28

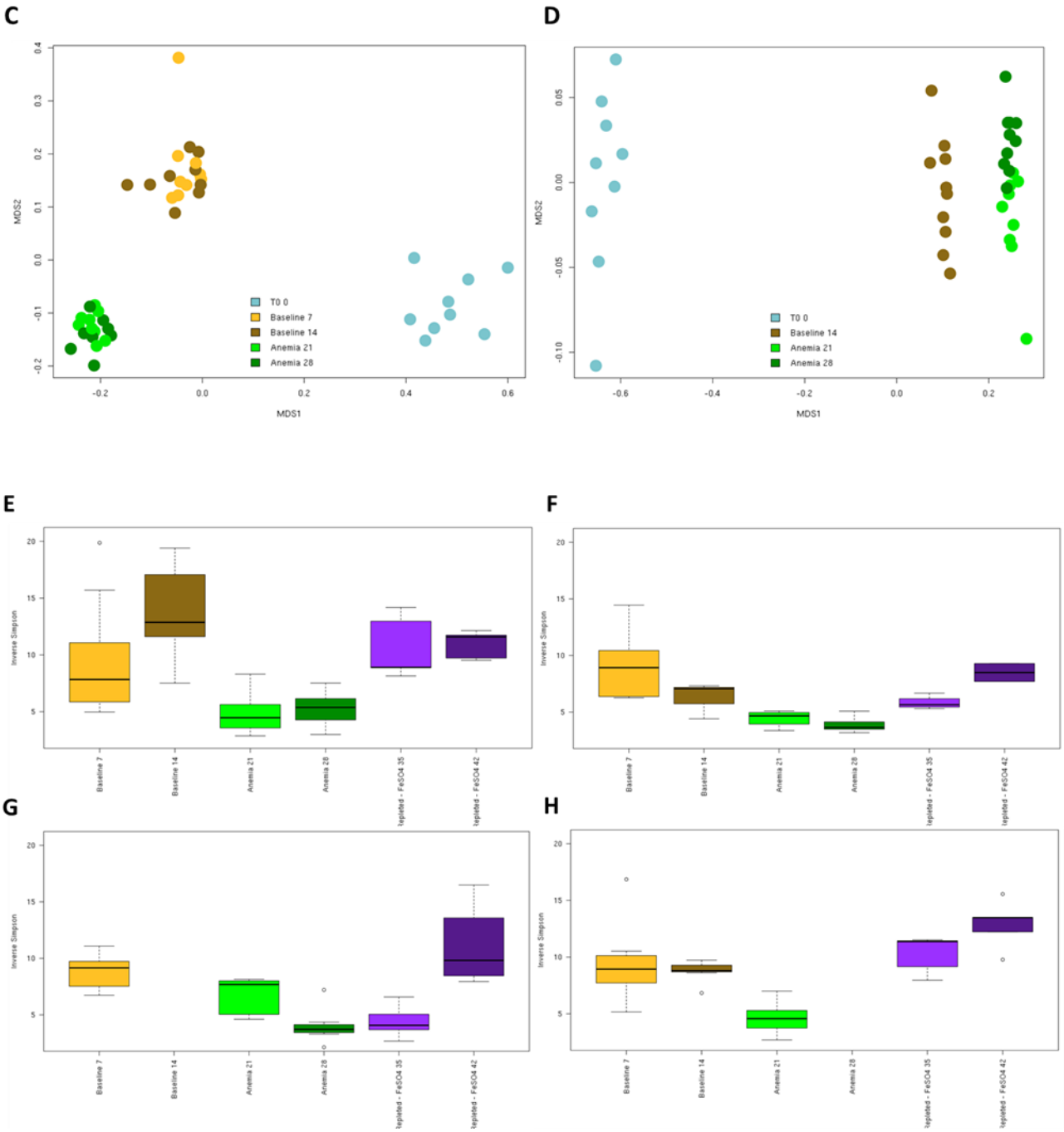
C
D
E
F
G
H
MDS1
MDS2
T0 0
Baseline 7
Baseline 14
Anemia 21
Anemia 28
Inverse Simpson
Baseline 7
Baseline 14
Anemia 21
Anemia 28
Repleted - FeSO4 35
Repleted - FeSO4 42

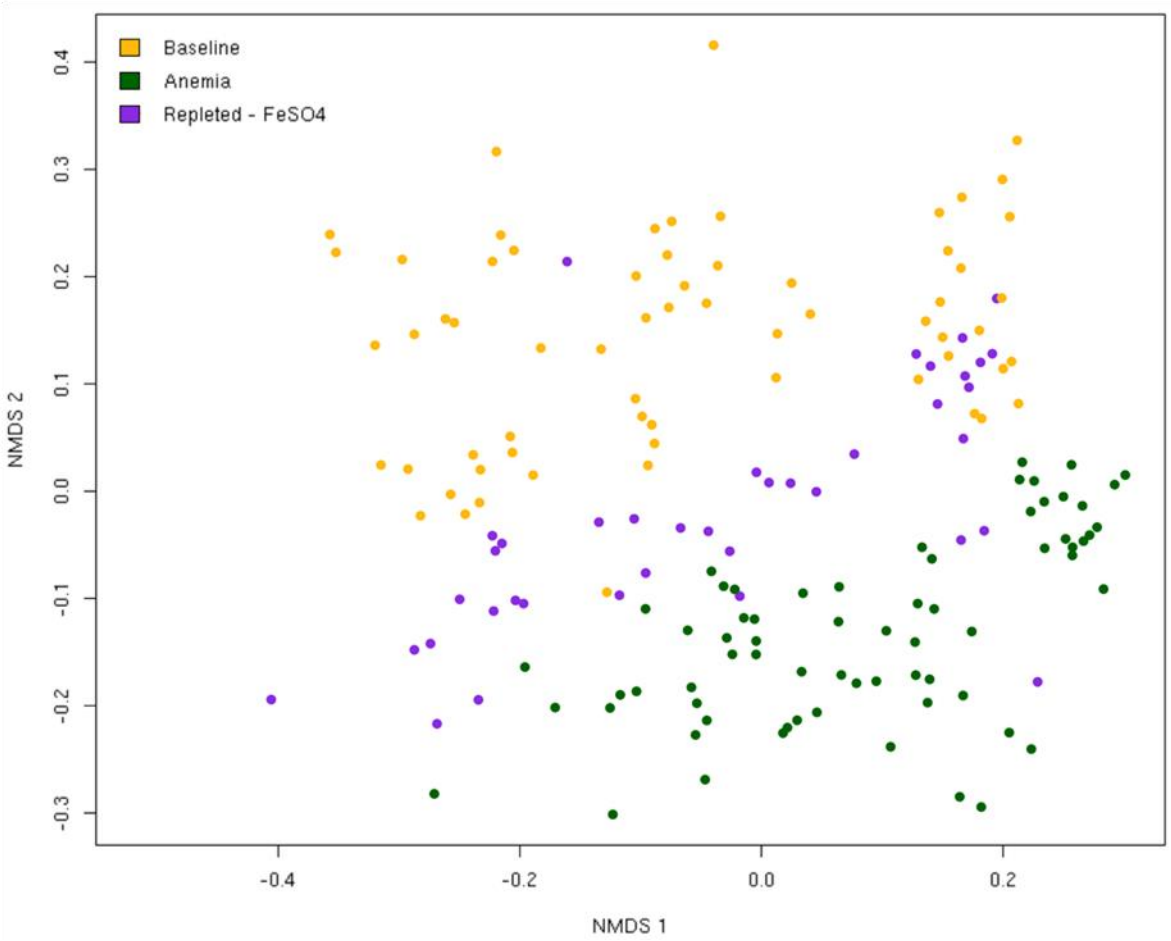

Figure 6. Diversity of the conventional mouse gut microbiome changes in response to iron bioavailability. A-B) α-diversity (richness and evenness distribution within a local community) decreases as iron becomes scarce in iron deficient mice (A: group 5, B: group 1). Mean ± 1 S.D. C-D) the conventional mouse gut microbiome shifts away from baseline in response to iron deficiency (C: group 5, D: group 1). E-H) α diversity increases upon iron repletion E: group 2, F: group 6, G: group 3, H: group 4 I) β-diversity shifts back towards baseline in iron repleted mice (groups 2,3,4,6). Yellow dots = groups 2,3,4,6 mice at the median of days 7 and 14 of baseline (0.328 mM iron sulfate heptahydrate and iron deficient chow), green dots = groups 2,3,4,6 mice at the median of 7 and 14 days on iron deficient chow and iron free water, purple dots = groups 2,3,4,6 mice at the median of 7 and 14 days of iron repletion. Effect of iron treatment on OTU distribution was tested using PERMANOVA in R and determined to be significant, $p < 0.05$.

The diversity of the gut microbial composition in conventional mice relative to the diversity of the same mice during different phases of treatment (β-diversity), shows a

distinct shift away from the baseline consortium in response to dietary iron deficiency in group 1 and 5 mice (**Figure 6C-D**). Groups 2,3,4, and 6 mice show a similar effect from baseline to anemia and repletion with iron sulfate where the diversity of the gut microbiome begins shifting back towards the baseline level of diversity **(Fig 6I, Fig 7A-D**). Non-metric multidimensional analysis (NMDS) demonstrates a visual example of the effect of iron treatment and time on β-diversity by showing variability between and within mouse groups represented by distance in a 2 dimensional space. Each circle represents the gut microbiome of a single mouse (male and female groups 2,3,4,6) and its distance relationship based on time and treatment phase to other mice. The distance between dots or mice indicates more diversity between each mouse at baseline. The distance traveled by mice going from baseline to anemia shows the level of difference in gut microbiome diversity in response to iron deficiency. Dots that are closer together indicate more similarity (and less diversity) between mice. Dots shift again from anemia to repletion phase demonstrating the effect of iron sulfate repletion to anemic mice and more similarity in the iron restored microbiome to the baseline microbiome. The gut microbiome at baseline did vary based on gender and age of mice however, the same trend in effect size between phases of treatment is similar regardless of age or gender (**Fig 7A-D**).

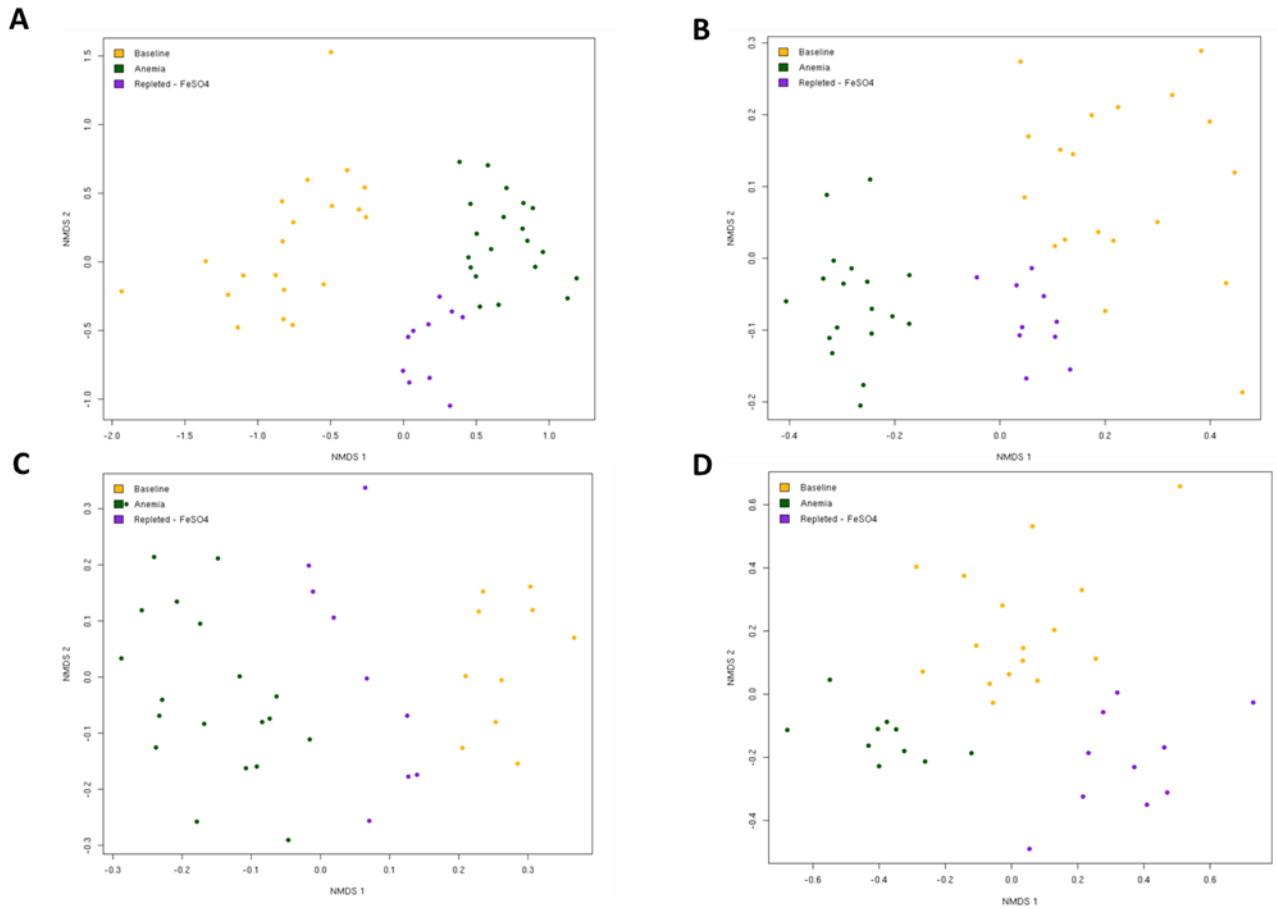

Figure 7. Gut microbiome diversity in male and female cohorts (groups 2, 3, 4, 6) over the course of iron treatment. Females (top) and males (bottom) β diversity of gut microbiome in each phase of treatment. A) group 2 B) group 6 C) group 3 D) group 4. Yellow dots = baseline (7 and/or 14 days on iron deficient chow and 0.32 mM $FeSO_4$ x $7H_2O$ in water), green dots = anemia (7 and/or 14 days on iron deficient chow and iron free water), purple dots = iron repletion (7 and/or 14 days on 0.32 mM $FeSO_4$ x $7H_2O$). Each dot represents the total OTU diversity in each mouse.

Over the course of iron treatment, OTUs either increased or decreased in abundance in response to iron bioavailability. Most notably there is an increase in bacteroidaceae(bacteroidetes), and bifidobacteriaceae(actinobacteria) in the anemia phase. Upon inorganic iron repletion, prevotellaceae and bifidobacteriaceae decrease in

abundance relative to the anemia phase. There is an observable decrease in anemia and repletion phases of lachnospiraceae (firmicutes), prevotellaceae (bacteroidetes), and bacteroidales or several unclassified members of the phylum bacteroidetes (**Figure 8**).

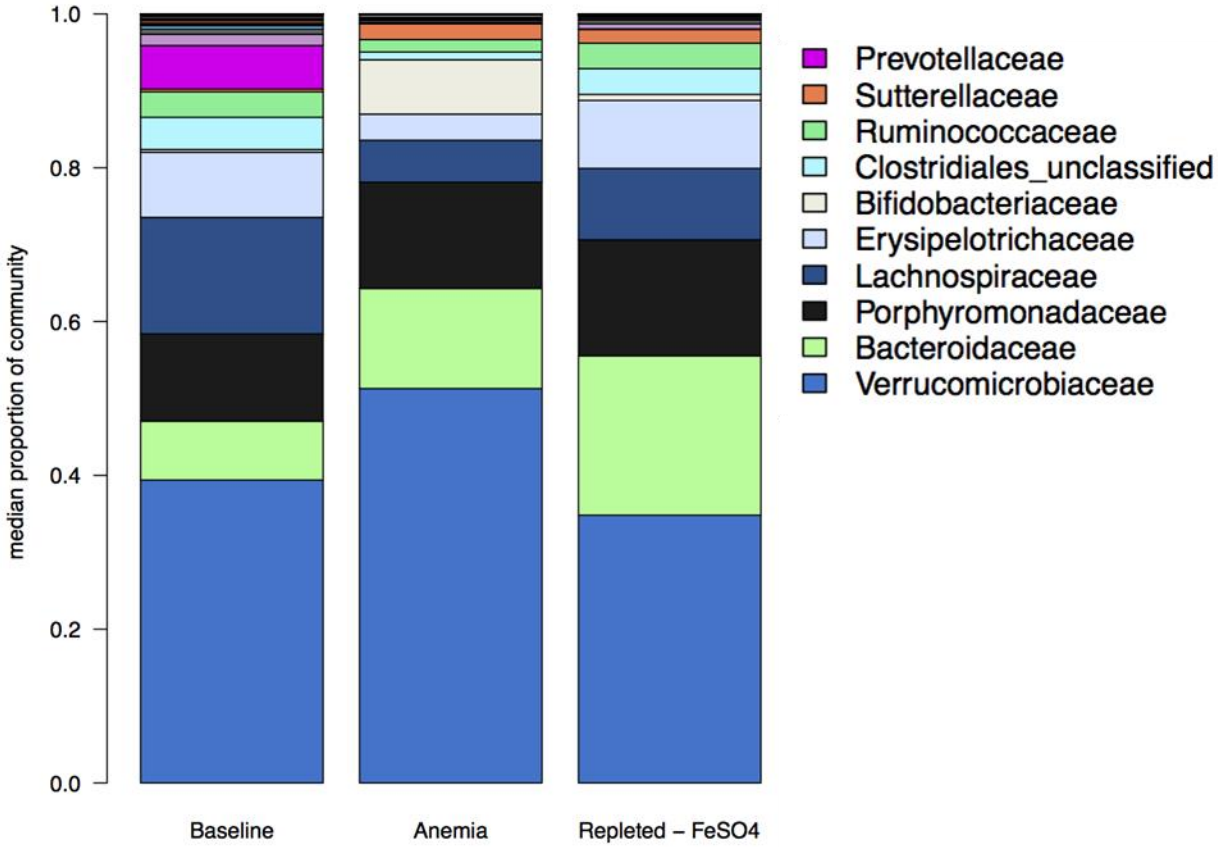

Figure 8. Changes in gut community composition (family level) in C57Bl/6 mice over the course of iron treatment. Bacterial families were compiled into a taxonomy bar chart based on median composition between all 4 groups of mice.

Further analysis of the median composition of OTUs common to groups 2,3,4, and 6, showed that there are seven unique OTUs in repleted mice that are not abundant in the baseline or anemia phases (**Figure 9**). There are seventeen OTUs unique to the

baseline that do not return after repletion and five OTUs that are unique to the anemia phase.

Figure 9. Number of OTUs unique to and shared in each phase of treatment (groups 2,3,4,6). The median representation of OTUs unique to each phase of treatment present in mice from groups 2,3,4, and 6.

Discussion

Total Iron in Serum and Pellets Suggests Iron Recycling by the Host During Iron Deficiency.

Mammalian iron metabolism involves recycling of circulated iron from the spleen as well as iron stores from the liver when a host is feeling iron deficient. Unlike serum iron levels, excreted iron, quantified from mouse feces, tells a different story. As mice

become iron deficient, the concentration of iron excreted decreases (**Figure 4B, 4D,** Table 3a-b). The concentration of excreted iron in inorganic iron repleted male and female cohorts does vary in the first week of repletion (Table 3b). The decrease of excreted iron during the anemia phase suggests that mice are retaining and recycling their iron stores in response to the nutrient deficiency and that the microbiome is not absorbing much iron. Coupled with the steady levels of iron in the serum (**Figure 4A, 4C**), it is reasonable to conclude that mice are adapting to insufficient dietary iron by depleting iron stores and recycling iron from the spleen. The purpose of characterizing the conventional mouse adaptation to anemia is to establish an iron deficient environment in a mammalian host and study the effect on the gut microbiome. The results above indicate that the mammalian host is feeling iron deficient after a two week period of dietary iron deficiency.

Iron Biomarker Expression in Iron
Deficient and Repleted Mice Depends on Source.

It is worthwhile to note that iron biomarkers are not up or down regulated in the same manner. For example, Dmt1 from the duodenum in anemic mice (**Figure 5A**) is more upregulated compared to ferroportin. Ferroportin is the iron exporter that sends iron to transferrin for circulation through the host. This transporter is known to be regulated by hepcidin, a hepatic hormone involved in the regulation of iron absorption. Hepcidin in turn is regulated by another transcription factor BMP6, which is turned on and off by stored iron levels[6]. Dcytb is also less expressed than Dmt1. It is unclear how many units of Dcytb are expressed on the cellular surface relative to Dmt1 but it is possible that

the ratio requires more dramatic upregulation of Dmt1 to Dcytb. It is also likely that there are other ferrireductases present on the cellular surface that may contribute to ferric iron reduction, resulting in lower expression of Dcytb relative to Dmt1[32]. Fold change number of the three iron biomarkers in the cecal tip of iron deficient mice (**Figure 5B**) is significantly higher than what is seen in the duodenum (**Figure 5A**). The cecal tip or cecum pouch is located between the small and large intestine and harbors a high density population of gut microbes. Its physiology and location are analogous to the human appendix but the cecum or cecal tip is much larger in comparison. The metabolic activity of both the host and resident microbes in the cecal tip may account for the increase in host iron biomarkers in this tissue. Additionally, the ascending colon or first segment of the large intestine is reported to have a much higher rate of metabolism compared to the mid or descending colon. It is also reported that there is a higher population of gut microbes in the mammalian large intestine than is found in the duodenum.

Summary of the Mammalian Host
Response to Dietary Iron Bioavailability.

Male and female mice (group 3,4, 6) made anemic and repleted with iron sulfate show down regulation of iron biomarkers in the duodenum and cecal tip tissues (**Figure 5C,D**) compared to female iron deficient mice (group 5) (**Figure 5A,B**). The objective of this paper was to explore the mouse gut microbial response to iron deficiency and repletion by defined iron sources. Characterizing the mammalian host response allows us to assess if the host environment is truly experiencing a state of iron deficiency and

whether the host environment can be rescued from iron deficiency by repletion with defined nutrient sources. Quantification of total iron in serum and pellets of both male and female mice suggest that the host is recycling iron as it becomes scarce in the diet. Expression of iron biomarkers in the duodenum and cecal tip suggest that iron deficient females are physiologically iron deficient and females and males repleted with iron sulfate are absorbing iron and restoring iron stores. Future studies by our group will further explore the physiological consequences of hemin as an alternative iron source to the host and gut microbiome.

Iron Bioavailability Influences the
Diversity of the Gut Microbiome in C57Bl/6 Mice.

Evaluation of microbial diversity specific to all cohorts of mice in one phase of iron treatment, known as α-diversity, was calculated using the inverse simpson index from the vegan package in R. The number of unique OTUs from all mice in each phase (richness) and the abundance of each OTU (evenness) is accounted for to provide a numerical ranking of microbial diversity on a numerical scale with one representing no diversity. The level of diversity in both male and female mice across each phase of treatment decreases as iron becomes scarce and increases again in iron sulfate repleted mice. It is important to note that α-diversity ranking does not indicate similar taxonomical composition. Even though β diversity increases for mice repleted with iron sulfate, the composition of the gut consortia does not match the baseline (**Figure 8**). It is interesting that the microbial population in iron sulfate repleted mice increases in α-

diversity to rank closely to the baseline (**Figure 6E-H**) but does not completely return to baseline based on clustering seen in **Figure 6I and 7A-D**. The baseline for NMDS or β diversity plots represents mice sustained on the iron-deficient chow and 17.8 ppm total iron in water over 7 and/or 14 days. Some fecal samples were unable to be sequenced at one time point for the baseline phase (group 3,4) or anemia phase (group 3). In order to assess the influence of the iron-deficient chow on the gut microbial composition, a cohort of five C57Bl/6 male mice were fed the iron-deficient chow for three weeks and fecal pellets were collected and processed for 16S rRNA sequencing. Results from gut microbial sequencing (data not shown) indicated that the gut microbiome stabilized well within the two-week time period allotted for the baseline phase as can be seen in the α and β diversity plots for groups 2-6. Results from **Figure 8** suggest that the shift in gut microbial composition after a period of dietary iron deficiency will result in an increase of richness and evenness but will not result in restoration of the microbiome to baseline upon repletion by a defined iron source within the 2 week period allotted.

Bacterial Diversity in the Gut May
Influence Repopulation in Response to Iron.

The distribution of bacteria classified by family was plotted based on median abundance in each phase of iron treatment for mouse groups 2-6 (**Figure 8**). There is an obvious shift in family composition between the baseline and anemia phases. Most notably, there is a significant increase in the bifidobacteriaceae family in the anemia phase. This family of bacteria have been reported in the literature to be iron scavengers

and are heavily populated in the guts of anemic infants[33]. As iron bioavailability becomes scarce, this family of bacteria increases, which might explain the increased expression of iron biomarkers in the cecal tip of the iron deficient host. As mentioned earlier, the cecal tip consists of a pouch adjacent to the end of the small intestine and the beginning of the large intestine and hosts a high density population of gut microbes. It would be reasonable to conclude that the iron scavenging activity by this family during a period of iron deficiency in the gut provides an advantage to survival. It has been demonstrated in the literature that commensal species within the family bifidobacteriaceae, are able to provide protection to a host via iron sequestration, preventing colonization by iron scavenging pathogens in the gut[34].

One study using simulated gut environments, showed that bacteroidaceae dwindle in population under low iron conditions and thrive when iron is bioavailable. Results reported here show that bacteroidaceae increase in number in response to iron deficiency. Lachnospiraceae have also been reported to decrease under low iron conditions both *in vitro* and *in vivo* which is consistent with results reported here. The symbiotic relationships between gut species are influenced by host environment, nutritional needs and the metabolic profiles produced by bacteria colonized in the gut. Fluctuations in abundance of bacterial taxa can also be explained by the symbiotic relationships that species within each family have under various nutritional conditions such as the influence of iron bioavailability. The composition of the microbiome during anemia is established primarily due to dietary iron deficiency. The repopulation and lack of complete restoration of the gut microbiome after repletion may be influenced both by the

composition of the gut microbiome during anemia as well as the concentration of dietary iron. There is much more to explore regarding the interactions of predominant bacteria in each phase of iron treatment but the major conclusion to be drawn from this study is that the bioavailability of iron drives the initial change in gut microbial composition, which may be accompanied by the relationships or interactions of remaining bacteria as another factor influencing repopulation (or increase in diversity) upon iron repletion.

The Venn diagram in **Figure 9** represents the median composition of OTUs unique to each phase for all mice (groups 2,3,4,6) to reflect what is seen in the median taxonomical distribution in **Figure 8**. The results from **Figure 9** further support the influence of the anemic gut microbiome composition on repopulation of specific OTUs in response to iron bioavailability in mice. While 17 OTUs disappear after the baseline phase, 13 are shared between baseline and repletion that are not present in the anemia phase. This supports the composition profile seen in **Figure 8**, where the taxonomy of repleted mice is similar to the baseline. However, for OTUs shared by all mice (groups 2,3,4,6), there are still 7 OTUs that are unique to the repletion phase, suggesting that the disrupted composition of the anemic microbiome influenced the abundance of those OTUs when iron became more bioavailable. In summary, the venn diagram in **Figure 9**, represents a median composition of unique OTUs shared by all mice in each phase, while **Figure 8** represents median abundance of OTUs shared by all mice in each phase. OTUs are considered unique to a phase if they surpass the cutoff for presence/absence as determined in R. Most unique OTUs were not belonging to a family that changed significantly from one phase to another (Table 6). For example, bifidobacteriaceae, while

not abundant in the baseline phase compared to the anemia phase still had a population of OTUs that were above the threshold for presence and are therefore not unique to the anemia and repletion phases. Unique OTUs are mostly unclassified species of families that populate in the repletion phase but are below the threshold for presence in the baseline phase. The loss of OTUs unique to the baseline phase and the addition of OTUs in the repletion phase further supports the changes in α- and β-diversity seen in **Figure 6**.

Physiological Contributions of
Predominant Bacterial Families in the Gut.

Lachnospiracea and bacteroidaceae include species that are known producers of short-chain fatty acids. These metabolites have been cited in the literature as major contributers to gut integrity, and multiple metabolic pathways in the mammalian host. As mentioned previously, bacteroidaceae have been cited in the literature to decrease in abundance in response to low iron availability however, our results show the opposite effect (anemia phase). The family of bacteroidaceae include several butyrate producing bacteria, which has been shown to be important for maintaining integrity of the epithelial lining in the lumen of the gut. It is worthwhile to note that although bacteroidaceae and suterellaceae include common inhabitants of human and other mammalian gut microbiomes, they also include species that are commonly isolated from human subjects with inflammatory bowel diseases[35,36]. While the mouse and human gut microbiomes are different below the phylum level, we can use these results to predict the changes that may occur in human gut microbiota during periods of iron deficiency and repletion with

two defined iron sources (iron sulfate and heme). We would expect an increase in α-diversity in heme repleted mice colonized with human gut microbiota since humans are adapted to using heme as a primary source of dietary iron when consuming a diet high in red meat. The consequence of heme repletion to the host with an iron deficient gut microbiome may result in increase of inflammation in the gut depending on the iron needs of remaining bacteria (many bacteria are not able to utilize extracellular heme as an iron source). Previous studies in the literature looking at the consequence of heme overload to the iron satisfied murine gut microbiome have suggested a strong correlation between dietary heme and inflammation in the gut[5].

Conclusions

The focus of this paper was to determine if a conventional mouse model could be characterized at both host and gut microbial levels for adaptation in response to iron bioavailability. As shown here, we have looked at the host response to iron deficiency and repletion by defined sources and determined that there is a shift in diversity and composition in the gut microbiome that is not fully recovered after repletion by iron. The purpose of characterizing this model was to provide a baseline to use in upcoming studies examining the effect of iron bioavailability on the human gut microbiome within a germ-free C57Bl/6 mouse host. Part of our future studies will include further examination of the effects of different iron sources (iron sulfate and heme) to both host and microbiome.

Table 1. Primer sequences used for iron biomarker expression

Marker	Forward (5'-> 3')	Reverse (5'-> 3')
Dmt1	CGGAGTCCTCATCACCATCG	CTGGCTGGGCTTCACTGTAA
Dcytb	GCAGCGGGCTCGAGTTTA	TTCCAGGTCCATGGCAGTCT
Ferroportin	TTGCAGGAGTCATTGCTGCTA	TGGAGTTCTGCACACCATTGAT
β-actin	AACCCTAAGGCCAACCGTGAA	TCACGCACGATTTCCCTCTCA

Table 2. Total circulated iron (ppm: mg/L) mean ± s.d. a) group 1 anemia, b,c)groups 2-4 repleted quantified by ICP-MS in mouse serum. Number of mice varies for some time points due to amount of sample being below the limit of detection of the ICP-MS instrument or loss of sample during collection. N = number of mice.

a)

	Anemia-group 1	SD	N
50 ppm Baseline wk2	255	23	9
4 ppm wk3	179	95	10
4 ppm wk4	303	42	10
50 ppm wk5			
50 ppm wk6			

b)

FeSO4-group 2	SD	N	FeSO4-group 3	SD	N	FeSO4-group 4	SD	N
297	66	5	335	11	5	279	54	5
310	61	5	305	44	5	204	130	5
321	48	5	309	46	5	317	46	5
362	11	4	289	78	5	326	22	5
398	23	4	277	38	5	346	18	5

Table 3. Total excreted iron (ppm: mg/kg) mean ± s.d. a) group 1 anemia, b) groups 2-4 repleted quantified by ICP-MS in mouse pellets. Number of mice varies for some time points due to amount of sample being below the limit of detection of the ICP-MS instrument or loss of sample during collection. N = number of mice.

a)

	Anemia-group 1	SD	N
50 ppm Baseline wk2	128	105	10
4 ppm wk3	48	49	6
50 ppm wk5			
50 ppm wk6			

b)

FeSO4-group 2	SD	N	FeSO4-group 3	SD	N	FeSO4-group 4	SD	N
155	80	5	83	39	5	90	50	5
34	2	3	37	16	5	37	5	4
267	50	5	146	40	5	146	26	5
82	53	5	95	26	4	210	162	5

Table 4. Fold change of iron biomarkers in duodenum mean ± s.d. a) group 5 anemia, b) groups 3-4, 6 repleted

a)

	Anemia-group 5	SD	N
Dmt-1	66	18	5
Ferroportin	17	5	5
Dcytb	32	22	5

b)

FeSO4-group 6	SD	N	FeSO4-group 3	SD	N	FeSO4-group 4	SD	N
0.7	0.2	5	7	7	5	0.2	0.2	3
7	2	5	2	1	5	1	0.5	3
2	0.7	5	4	5	5	0.9	0.6	3

Table 5. Fold change of iron biomarkers in cecal tip mean ± s.d. a) group 5 anemia, b) groups 3-4, 6 repleted

a)

	Anemia-group 5	SD	N
Dmt-1	298	93	5
Ferroportin	134	44	5
Dcytb	318	183	5

b)

FeSO4-group 6	SD	N	FeSO4-group 3	SD	N	FeSO4-group 4	SD	N
1	0.8	5	22	9	5	0.3	0.05	4
1	2	5	5	1	5	3	2	4
0.3	0.4	5	3	0.7	5	1	0.5	4

Table 6. Classification of OTUs unique to each phase of iron treatment in mice (groups 2,3,4,6) a) Baseline b) Anemia c) Repleted

a)

OTU_ID	Family	Genus
Otu0009	Erysipelotrichaceae	unclassified
Otu0021	Porphyromonadaceae	unclassified
Otu0032	Porphyromonadaceae	unclassified
Otu0041	Desulfovibrionaceae	unclassified
Otu0045	Lachnospiraceae	unclassified
Otu0046	Porphyromonadaceae	unclassified
Otu0049	Ruminococcaceae	unclassified
Otu0052	Porphyromonadaceae	unclassified
Otu0055	Rikenellaceae	Alistipes
Otu0057	Lachnospiraceae	Clostridium_XlVb
Otu0061	Porphyromonadaceae	Barnesiella
Otu0069	Lachnospiraceae	unclassified
Otu0086	Ruminococcaceae	unclassified
Otu0099	Lachnospiraceae	unclassified
Otu0100	Lachnospiraceae	unclassified
Otu0105	Ruminococcaceae	unclassified
Otu0116	Ruminococcaceae	unclassified

b)

OTU_ID	Family	Genus
Otu0020	Lachnospiraceae	Acetatifactor
Otu0022	Rikenellaceae	Alistepes
Otu0034	Rhodospirillaceae	unclassified
Otu0058	Porphyromonadaceae	unclassified

Otu0106	Lachnospiraceae	Acetatifactor

c)

OTU_ID	Family	Genus
Otu0017	Erysipelotrichaceae	unclassified
Otu0028	Bacteroidaceae	Bacteroides
Otu0031	Erysipelotrichaceae	unclassified
Otu0064	Lachnospiraceae	unclassified
Otu0070	Lachnospiraceae	unclassified
Otu0085	Lachnospiraceae	unclassified
Otu0026	Porphyromonadaceae	unclassified

REFERENCES CITED

1. Frey PA, Reed GH: **The ubiquity of iron**. *ACS Chem Biol* 2012, **7**:1477-1481.
2. Pantopoulos K, Porwal SK, Tartakoff A, Devireddy L: **Mechanisms of mammalian iron homeostasis**. *Biochemistry* 2012, **51**:5705-5724.
3. Anderson CP, Shen M, Eisenstein RS, Leibold EA: **Mammalian iron metabolism and its control by iron regulatory proteins**. *Biochim Biophys Acta* 2012, **1823**:1468-1483.
4. Puntarulo S: **Iron, oxidative stress and human health**. *Mol Aspects Med* 2005, **26**:299-312.
5. N IJ, Derrien M, van Doorn GM, Rijnierse A, van den Bogert B, Muller M, Dekker J, Kleerebezem M, van der Meer R: **Dietary heme alters microbiota and mucosa of mouse colon without functional changes in host-microbe cross-talk**. *PLoS One* 2012, **7**:e49868.
6. Ganz T: **Systemic iron homeostasis**. *Physiol Rev* 2013, **93**:1721-1741.
7. Hurrell R, Egli I: **Iron bioavailability and dietary reference values**. *Am J Clin Nutr* 2010, **91**:1461S-1467S.
8. Enculescu M, Metzendorf C, Sparla R, Hahnel M, Bode J, Muckenthaler MU, Legewie S: **Modelling Systemic Iron Regulation during Dietary Iron Overload and Acute Inflammation: Role of Hepcidin-Independent Mechanisms**. *PLoS Comput Biol* 2017, **13**:e1005322.
9. Steinbicker AU, Muckenthaler MU: **Out of balance--systemic iron homeostasis in iron-related disorders**. *Nutrients* 2013, **5**:3034-3061.
10. **<._2007_Dailey HsHemH structures_mechanism.pdf>**.
11. Costea PI, Hildebrand F, Arumugam M, Backhed F, Blaser MJ, Bushman FD, de Vos WM, Ehrlich SD, Fraser CM, Hattori M, et al.: **Enterotypes in the landscape of gut microbial community composition**. *Nat Microbiol* 2018, **3**:8-16.
12. Canny GO, McCormick BA: **Bacteria in the intestine, helpful residents or enemies from within?** *Infect Immun* 2008, **76**:3360-3373.
13. Lloyd-Price J, Abu-Ali G, Huttenhower C: **The healthy human microbiome**. *Genome Med* 2016, **8**:51.
14. Macfarlane S, Steed H, Macfarlane GT: **Intestinal bacteria and inflammatory bowel disease**. *Crit Rev Clin Lab Sci* 2009, **46**:25-54.
15. Morrison DJ, Preston T: **Formation of short chain fatty acids by the gut microbiota and their impact on human metabolism**. *Gut Microbes* 2016, **7**:189-200.
16. Slingerland AE, Schwabkey Z, Wiesnoski DH, Jenq RR: **Clinical Evidence for the Microbiome in Inflammatory Diseases**. *Front Immunol* 2017, **8**:400.
17. Louis P, Flint HJ: **Diversity, metabolism and microbial ecology of butyrate-producing bacteria from the human large intestine**. *FEMS Microbiol Lett* 2009, **294**:1-8.

18. Vazquez-Gutierrez P, de Wouters T, Werder J, Chassard C, Lacroix C: **High Iron-Sequestrating Bifidobacteria Inhibit Enteropathogen Growth and Adhesion to Intestinal Epithelial Cells In vitro**. *Front Microbiol* 2016, **7**:1480.
19. Kortman GA, Raffatellu M, Swinkels DW, Tjalsma H: **Nutritional iron turned inside out: intestinal stress from a gut microbial perspective**. *FEMS Microbiol Rev* 2014, **38**:1202-1234.
20. Krewulak KD, Vogel HJ: **Structural biology of bacterial iron uptake**. *Biochim Biophys Acta* 2008, **1778**:1781-1804.
21. Fischbach MA, Lin H, Liu DR, Walsh CT: **How pathogenic bacteria evade mammalian sabotage in the battle for iron**. *Nat Chem Biol* 2006, **2**:132-138.
22. Correnti C, Strong RK: **Mammalian siderophores, siderophore-binding lipocalins, and the labile iron pool**. *J Biol Chem* 2012, **287**:13524-13531.
23. Sassone-Corsi M, Chairatana P, Zheng T, Perez-Lopez A, Edwards RA, George MD, Nolan EM, Raffatellu M: **Siderophore-based immunization strategy to inhibit growth of enteric pathogens**. *Proc Natl Acad Sci U S A* 2016, **113**:13462-13467.
24. **<._2016 Hobbs_ HemQ generates ROS.pdf>**.
25. Haley KP, Skaar EP: **A battle for iron: host sequestration and Staphylococcus aureus acquisition**. *Microbes Infect* 2012, **14**:217-227.
26. Ley RE, Backhed F, Turnbaugh P, Lozupone CA, Knight RD, Gordon JI: **Obesity alters gut microbial ecology**. *Proc Natl Acad Sci U S A* 2005, **102**:11070-11075.
27. Lesuisse E: **Iron use for haeme synthesis is under control of the yeast frataxin homologue (Yfh1)**. *Human Molecular Genetics* 2003, **12**:879-889.
28. Kim J, Buckett PD, Wessling-Resnick M: **Absorption of manganese and iron in a mouse model of hemochromatosis**. *PLoS One* 2013, **8**:e64944.
29. Deschemin JC, Noordine ML, Remot A, Willemetz A, Afif C, Canonne-Hergaux F, Langella P, Karim Z, Vaulont S, Thomas M, et al.: **The microbiota shifts the iron sensing of intestinal cells**. *FASEB J* 2016, **30**:252-261.
30. **<._2017-Dailey-Multiple pathways to heme bio_Micor Mol Rev.pdf>**.
31. **<._Yuan_2016_Heme cell reporters PNAS.pdf>**.
32. **<1997_vonEiff_hemB_SCV.pdf>**.
33. Vazquez-Gutierrez P, Lacroix C, Jaeggi T, Zeder C, Zimmerman MB, Chassard C: **Bifidobacteria strains isolated from stools of iron deficient infants can efficiently sequester iron**. *BMC Microbiol* 2015, **15**:3.
34. O'Callaghan A, van Sinderen D: **Bifidobacteria and Their Role as Members of the Human Gut Microbiota**. *Front Microbiol* 2016, **7**:925.
35. Wexler HM: **Bacteroides: the good, the bad, and the nitty-gritty**. *Clin Microbiol Rev* 2007, **20**:593-621.
36. Hiippala K, Kainulainen V, Kalliomaki M, Arkkila P, Satokari R: **Mucosal Prevalence and Interactions with the Epithelium Indicate Commensalism of Sutterella spp**. *Front Microbiol* 2016, **7**:1706.

APPENDIX

Each mouse cohort consisted of ten mice (see materials and methods) split into 5 mice per cage. Both subgroups of five mice in each cohort were placed on the same timeline for the baseline and anemia phases of treatment. Upon repletion, one cage of five mice were repleted with iron sulfate as described in the main text and the other five mice were repleted with heme. This experimental approach was carried out for mouse groups 2, 3, 4, and 6. Due to differences in the amount of total iron found in iron sulfate versus heme, we are currently optimizing the method for heme repletion to reflect the same amount of total iron upon repletion as mice receiving iron sulfate. The following results represent the host and gut microbiome response to heme repletion after iron deficiency where mice were receiving 0.076 mM hemin chloride in their water supply.

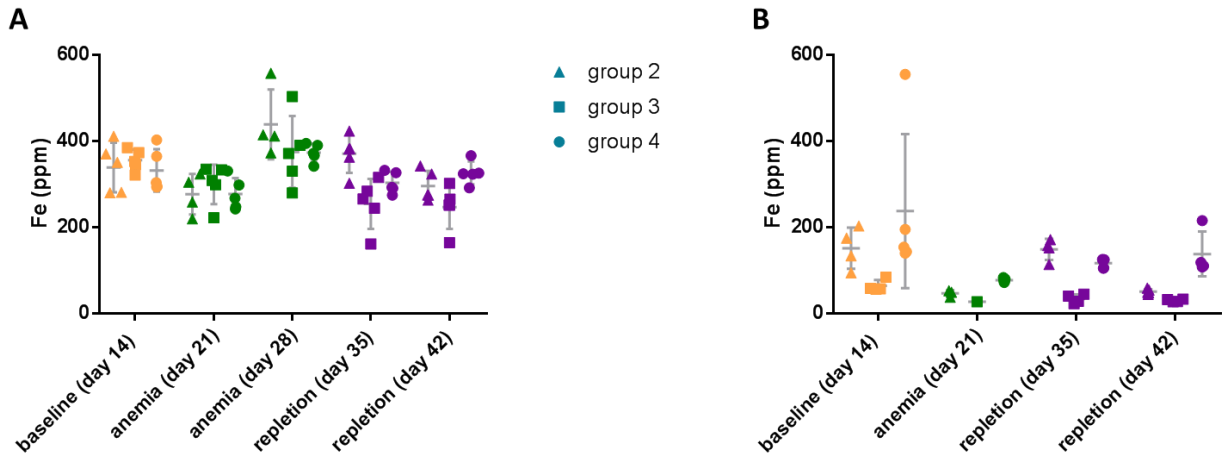

Figure A1. Total iron in serum and fecal pellets in heme repleted mice quantified by ICP-MS. A) Total serum iron in male and female mice over each phase of iron treatment. B) Total excreted iron in male and female mice over each phase of iron treatment.

Heme repleted mice were placed on the same diet regimen as iron sulfate repleted mice (see main text). Serum iron shows similar trends seen in iron sulfate repleted mice, where total iron in the serum fluctuates slightly on the second week of iron deficiency but levels out similar to the total serum iron seen at the baseline (**Figure A1.A,** Table A1.a). Baseline corresponds to the two week period of being on the iron deficient chow with 0.32 mM iron sulfate heptahydrate supplemented in the water supply. Repletion with 0.076 mM hemin chloride in the water results in some increase in excreted iron for groups 2 and 4 (**Figure A1.B,** Table A1.b). In comparison, iron sulfate repleted mice showed a much higher amount of excreted iron during this phase. Because the amount of

total iron form hemin chloride is less than the total iron from iron sulfate heptahydrate, we are unable to conclude whether this response is due to the source of iron being used or if it is a result of not having enough total iron during repletion.

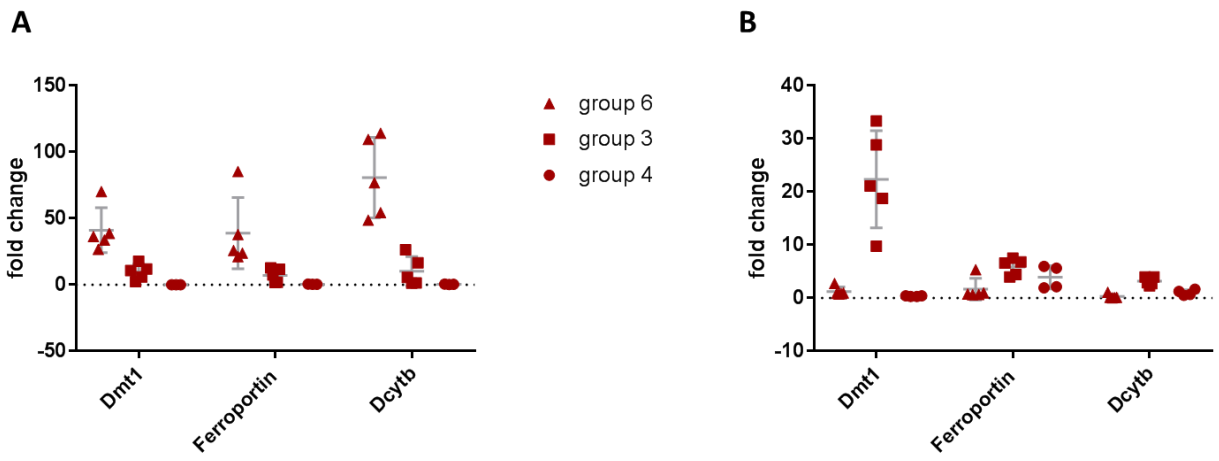

Figure A2. Fold change expression of iron biomarkers in small intestine of heme repleted mice. A) fold change expression of iron biomarkers in the duodenum of male and female mice 14 days after repletion with heme. B) fold change expression of iron biomarkers in the cecal tip of male and female mice 14 days after repletion with heme.

Group 6 females showed a much higher fold change expression of iron biomarkers in the duodenum (**Figure A2.A,** Table A2.a) after two weeks of hemin chloride repletion (4.25 mg/L total iron, 0.076 mM hemin chloride). When compared to the expression of biomarkers in the duodenum of anemic mice (group 5, **Figure 5A**), group 6 heme repleted mice show higher fold change. In contrast the expression of iron biomarkers in the cecal tip for group 6 heme repleted mice (**Figure A2.B,** Table A2.b) is much lower than that of anemic mice (**Figure 5B**). Groups 3 and 4 heme repleted mice (**Figure 2A.A-B**) showed a decrease in fold change of iron biomarkers in both locations of the small intestine compared to anemic mice (**Figure 5A,B**).

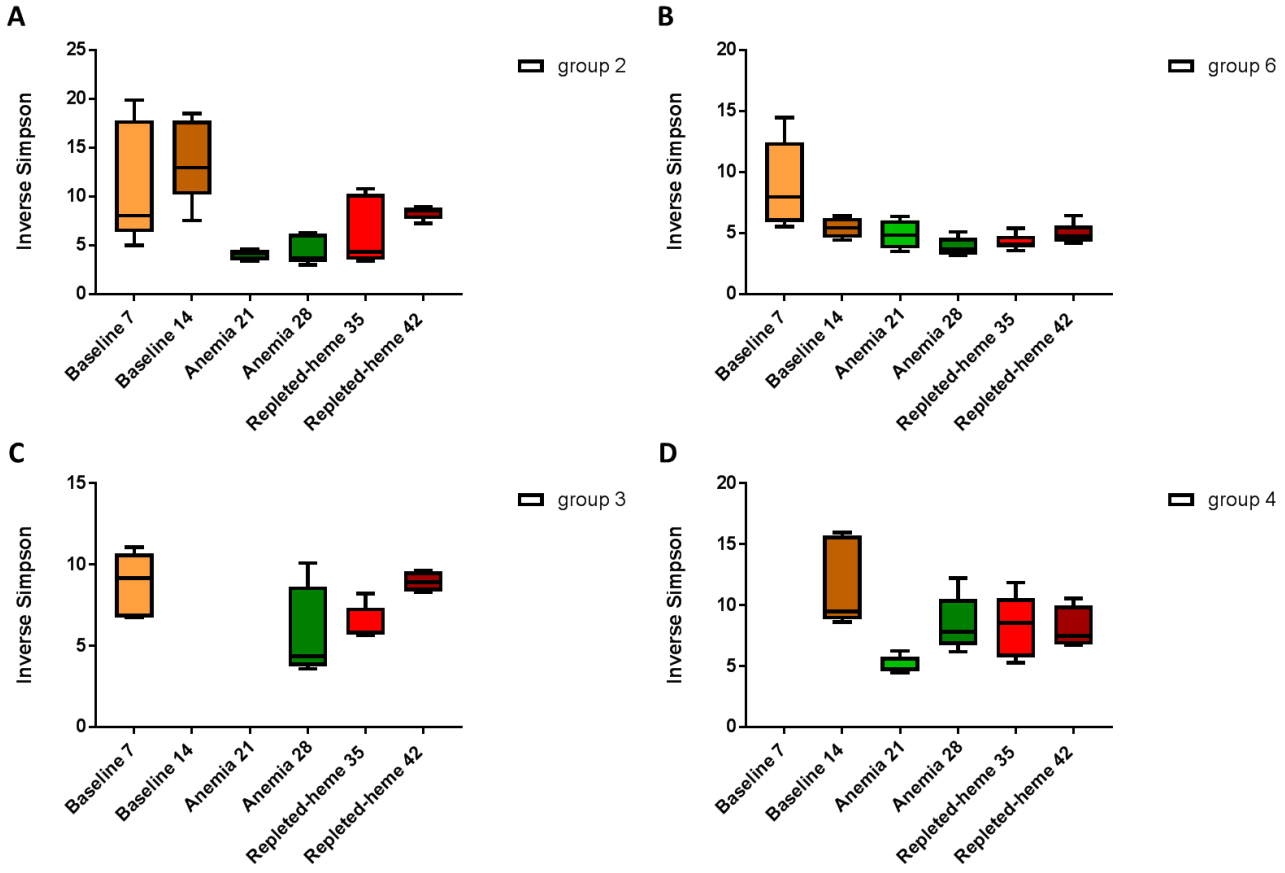

Figure A3. α-diversity of mouse gut microbiomes (groups 2,3,4,6) before and after heme repletion. Inverse Simpson indeces were plotted for heme repleted mice from groups 2,3,4,6 before and after anemia and repletion by heme. A) group 2, B) group 6, C) group 3, D) group 4.

The above trends in α-diversity (**Figure A3.A-D**) show the initial decrease in response to iron depletion in female groups (2, 6) and male group 4 but not male group 3. Repletion by heme shows very little increase in diversity compared to the spread in diversity during anemia for all groups of mice.

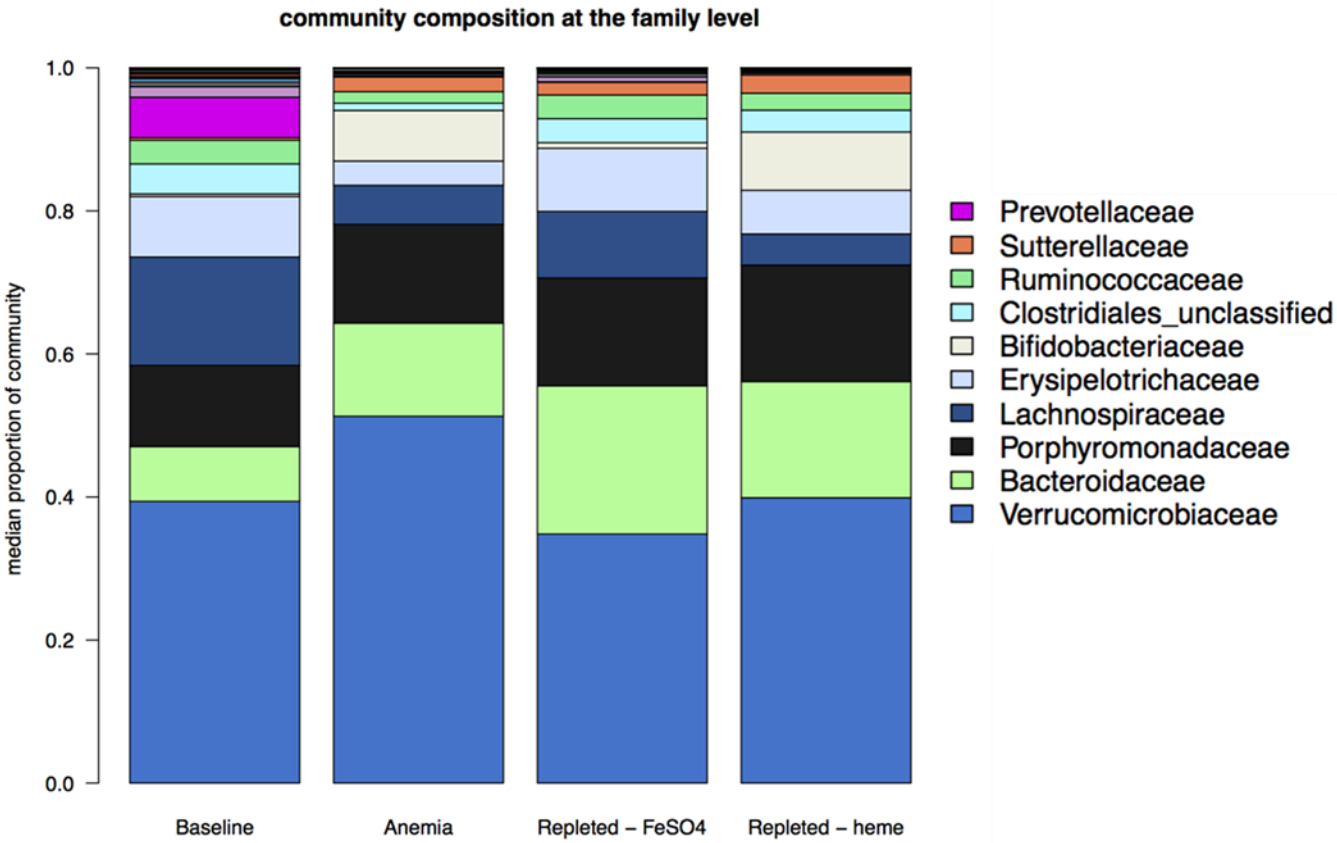

Figure A4. Median composition of gut microbiome (family level) in mice (groups 2,3,4,6) in response to iron bioavailability.

Median composition of the gut microbiome in heme repleted mice more closely resembles the composition during the anemia phase (**Figure A4**). In contrast, the iron sulfate repleted mice are more similar in composition to the baseline than the anemia phase consortium. As previously discussed, we are unable to conclude whether this is a result of iron source or amount of total iron repleted to mice receiving hemin chloride.

Table A1. Total iron (ppm) in serum (mg/L) (a) and pellets (mg/kg) (b) in male and female mice repleted with heme. Mean ± 1 s.d.

a)

Heme-group 2	SD	N	Heme-group 3	SD	N	Heme-group 4	SD	N
338	57	5	355	24	5	331	49	5
276	46	4	298	45	5	276	36	5
438	80	4	374	83	5	372	21	5
370	44	5	253	57	5	302	24	5
295	34	5	246	50	5	325	26	5

b)

Heme-group 2	SD	N	Heme-group 3	SD	N	Heme-group 4	SD	N
151	47	4	64	13	4	93	67	5
46	7	3	27	0	1	37	1	5
148	24	4	33	10	4	48	5	5
50	5	5	30	3	4	68	30	4

Table A2. Fold change expression of iron biomarkers in duodenum (a) and cecal tip (b) in male and female mice repleted with heme. Mean ± 1 s.d.

a)

Heme-group 6	SD	N	Heme-group 3	SD	N	Heme-group 4	SD	N
41	16	5	9	5	5	0.1	0.05	3
38	26	5	7	5	5	0.4	0.08	3
80	30	5	10	10	5	0.4	0.1	3

b)

Heme-group 6	SD	N	Heme-group 3	SD	N	Heme-group 4	SD	N
1	0.4	5	23	16	5	0.6	0.2	4
1	0.3	5	7	4	5	3	1	4
0.1	0.1	5	3	2	5	0.7	0.3	4